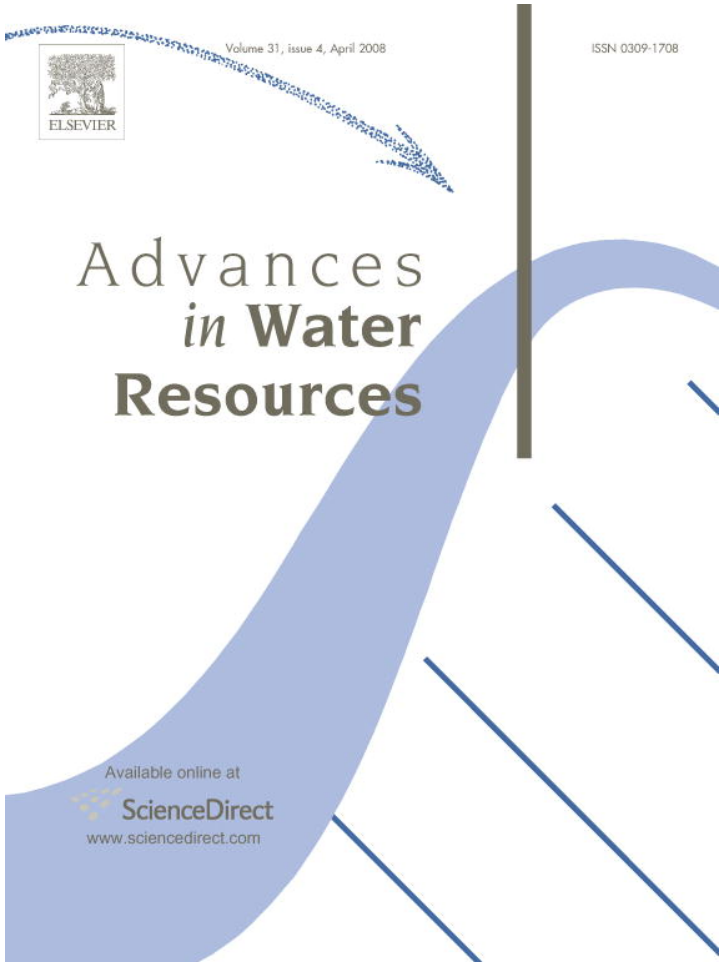

Available online at www.sciencedirect.com
ScienceDirect
Advances in Water Resources 31 (2008) 599–608
Advances in Water Resources
www.elsevier.com/locate/advwatres

Flow based oversampling technique for multiscale finite element methods

J. Chu [a], Y. Efendiev [b,*], V. Ginting [c], T.Y. Hou [a]

[a] Applied Mathematics, Caltech, Pasadena, CA 91125, United States
[b] Department of Mathematics, Texas A&M University, College Station, TX 77843-3368, United States
[c] Department of Mathematics, University of Wyoming, Laramie, WY 82071, United States

Received 11 June 2007; received in revised form 6 November 2007; accepted 15 November 2007
Available online 5 December 2007

Abstract

Oversampling techniques are often used in porous media simulations to achieve high accuracy in multiscale simulations. These methods reduce the effect of artificial boundary conditions that are imposed in computing local quantities, such as upscaled permeabilities or basis functions. In the problems without scale separation and strong non-local effects, the oversampling region is taken to be the entire domain. The basis functions are computed using single-phase flow solutions which are further used in dynamic two-phase simulations. The standard oversampling approaches employ generic global boundary conditions which are not associated with actual flow boundary conditions. In this paper, we propose a flow based oversampling method where the actual two-phase flow boundary conditions are used in constructing oversampling auxiliary functions. Our numerical results show that the flow based oversampling approach is several times more accurate than the standard oversampling method. We provide partial theoretical explanation for these numerical observations.

Keywords: Multiscale; Finite volume; Oversampling; Upscaling; Two-phase flow

1. Introduction

The high degree of variability and multiscale nature of formation properties such as permeability pose significant challenges for subsurface flow modeling. Geological characterizations that capture these effects are typically developed at scales that are too fine for direct flow simulation, so techniques are required to enable the solution of flow problems in practice. Upscaling procedures have been commonly applied for this purpose and are effective in many cases (see [28,26,19] for reviews and discussion). More recently, a number of multiscale finite element (e.g., [20,10,3,1,2,17]) and finite volume [22,23] approaches have been developed and successfully applied for problems of this type.

Our purpose in this paper is to propose a new oversampling strategy in constructing multiscale basis functions within the framework of multiscale finite element method (MsFEM). The MsFEM was first introduced in [20]. Its main idea is to incorporate the small-scale information into finite element basis functions and capture their effect on the large-scale via finite element computations. There are a number of multiscale numerical methods (or framework) with similar general objective, such as generalized finite element methods [5], residual free bubbles [27], variational multiscale method [21], multiscale finite element method (MsFEM) [20], two-scale finite element methods [24], two-scale conservative subgrid approaches [3], heterogeneous multiscale method (HMM) [16], and multiscale mortar methods [4]. We remark that special basis functions in finite element methods have been used earlier in [6]. Multiscale finite element methodology has been modified and successfully applied to two-phase flow simulations in [22,23] and later in [10,1].

* Corresponding author. Tel.: +1 979 845 1972.
E-mail address: efendiev@math.tamu.edu (Y. Efendiev).

0309-1708/$ - see front matter © 2007 Elsevier Ltd. All rights reserved.
doi:10.1016/j.advwatres.2007.11.005

Most multiscale methods presented to date have applied local calculations for the determination of basis functions (or, in the case of variational multiscale methods [3], subgrid integrals). Though effective in many cases, the accuracy of these local calculations may deteriorate for problems in which global effects are crucial. The importance of global information has been illustrated within the context of upscaling procedures in recent investigations [9,8].

These studies have shown that the use of global information in the calculation of the upscaled parameters can significantly improve the accuracy of the resulting coarse model.

In this paper, we propose a flow based oversampling method. The main idea of oversampling techniques is to use solutions of the underlying single-phase flow equation in larger domains for computing the basis functions. These basis functions are used in the two-phase flow simulations with varying (dynamic) mobility. Oversampling techniques reduce the effect of artificial boundary conditions that are often imposed in computing local quantities, such as upscaled permeabilities or basis functions. When there is no scale separation, the oversampling region is taken to be the entire domain. Typically, generic boundary conditions are used to compute the auxiliary oversampling functions. These boundary conditions do not reflect the actual two-phase flow boundary conditions which can have large effect in the simulations. In particular, when two-phase flow boundary conditions contain some type of singularities, the single-phase flow solutions obtained using generic boundary conditions are not sufficient to represent these effects. For this reason, one needs to incorporate the actual two-phase flow boundary conditions. In the proposed flow based oversampling method, we take one (or more) auxiliary oversampling functions to be the solution of single-phase flow equations with original (two-phase flow) boundary information. We present a partial analysis which demonstrates the importance of using the actual boundary conditions. Moreover, our analysis explains when one needs to use the actual two-phase flow boundary conditions which is associated to the "singularity" in the boundary conditions of two-phase flows.

To illustrate the performance of this new strategy, we present several representative numerical results. In particular, comparison between the flow based and standard oversampling is made for typical two-phase flow and transport simulations. In our numerical results, we use the permeability fields from the SPE comparative project [12]. These permeability fields are channelized and difficult to upscale. In particular, due to channelized nature of these permeability fields, the non-local effects are important and, often, some type of limited global information is used in multiscale simulations (e.g., [17,15]). In our simulations, we test various viscosity ratios and compare integrated quantities, such as oil production rate and total flow rate, as well as the saturation errors at some time instances. In all cases, we observe that the flow based oversampling methods are more accurate and, in almost all the cases we consider, it gives several orders of improvement.

The paper is organized in the following way. In the next section we give some preliminaries explaining the two-phase flow fine-scale model and the multiscale finite volume element method (MsFVEM). In Section 3, we present the flow based oversampling approach and analysis. Finally, in Section 4, the numerical results are presented.

2. Preliminaries

We consider two-phase flow in a reservoir Ω under the assumption that the displacement is dominated by viscous effects; i.e., we neglect the effects of gravity, compressibility, and capillary pressure. Porosity is assumed to be constant. In this flow problem, the two phases are water and oil, designated by subscripts w and o, respectively. We write Darcy's law, with all quantities dimensionless, for each phase as follows:

$$\mathbf{v}_j = -\frac{k_{rj}(S)}{\mu_j}\mathbf{k}\cdot\nabla p, \tag{2.1}$$

where $\mathbf{v}_j$ is the phase velocity, $\mathbf{k}$ is the permeability tensor, k_{rj} is the relative permeability to phase j ($j = o, w$), S is the water saturation (volume fraction), p is pressure and μ_j is the viscosity of phase j ($j = o, w$). In this work, a single set of relative permeability curves is used and $\mathbf{k}$ is assumed to be a diagonal tensor. Combining Darcy's law with a statement of conservation of mass allows us to express the governing equations in terms of the so-called pressure and saturation equations:

$$\nabla\cdot(\lambda(S)\mathbf{k}\cdot\nabla p) = h, \tag{2.2}$$

$$\frac{\partial S}{\partial t} + \mathbf{v}\cdot\nabla f(S) = h_{\mathrm{w}}, \tag{2.3}$$

where λ is the total mobility, f is the fractional flow of water, $h = h_{\mathrm{w}} + h_{\mathrm{o}}$ is a source/sink term and $\mathbf{v}$ is the total velocity, which are respectively given by:

$$\lambda(S) = \frac{k_{\mathrm{rw}}(S)}{\mu_{\mathrm{w}}} + \frac{k_{\mathrm{ro}}(S)}{\mu_{\mathrm{o}}}, \quad f(S) = \frac{k_{\mathrm{rw}}(S)/\mu_{\mathrm{w}}}{k_{\mathrm{rw}}(S)/\mu_{\mathrm{w}} + k_{\mathrm{ro}}(S)/\mu_{\mathrm{o}}}, \tag{2.4}$$

$$\mathbf{v} = \mathbf{v}_{\mathrm{w}} + \mathbf{v}_{\mathrm{o}} = -\lambda(S)\mathbf{k}\cdot\nabla p. \tag{2.5}$$

The above descriptions are referred to as the fine model of the two-phase flow problem. Typical boundary conditions for (2.2) considered in this paper are fixed pressure at some portions of the boundary and no-flow on the rest of the boundary. For the saturation Eq. (2.3), we impose $S = 1$ on the inflow boundaries. For simplicity, in further analysis we will assume that $h_{\mathrm{w}} = h_{\mathrm{o}} = 0$ so that $h = 0$.

The upscaling of two-phase flow systems is discussed by many authors [11,7,14]. In most upscaling procedures, the coarse-scale pressure equation is of the same form as the fine-scale Eq. (2.2), but with an equivalent grid block permeability tensor $\mathbf{k}^*$ replacing $\mathbf{k}$. For a given coarse-scale grid block, the tensor $\mathbf{k}^*$ is generally computed through

the solution of the pressure equation over the local fine-scale region corresponding to the particular coarse block [13]. Coarse-grid $\mathbf{k}^*$ computed in this manner has been shown to provide accurate solutions to the coarse-grid pressure equation. As we mentioned in Introduction, for channelized porous media, the global information can be used in calculation of effective coarse-grid permeability [9], but these upscaling approaches are not exact at the initial time.

2.1. Multiscale finite volume element procedure

In this section, we briefly recall multiscale finite volume element method. We denote by $\mathscr{K}^h$ the set of coarse elements (rectangles in this case) K. The quantity $\boldsymbol{\xi}_K$ indicates the center of coarse element K. Element K is divided into four rectangles of equal area by connecting $\boldsymbol{\xi}_K$ to the midpoints of the element edges. These quadrilaterals are denoted by $K_{\boldsymbol{\xi}}$, where $\boldsymbol{\xi} \in Z_h(K)$, are the vertices of K. We designate $Z_h = \bigcup_K Z_h(K)$ and $Z_h^0 \subset Z_h$ the vertices which do not lie on the Dirichlet boundary of Ω. The control volume $V_{\boldsymbol{\xi}}$ is defined as the union of the quadrilaterals $K_{\boldsymbol{\xi}}$ sharing the vertex $\boldsymbol{\xi}$. The grid comprised of elements K (solid squares in Fig. 1) is sometimes referred to as the primal grid and the grid defined by $V_{\boldsymbol{\xi}}$ (dashed square in Fig. 1) as the dual grid. In our procedure we compute pressure at the vertices of the primal grid. This differs from the approach of [22,23] in which pressure is computed at the centroids of the primal grid blocks. This also leads to a different treatment of global boundary conditions.

The goal of the MsFVEM is to determine coarse scale basis functions that incorporate the fine scale information in the underlying permeability description. The technique applied here follows the multiscale finite element method of [20], as the basis functions are determined from the solution of the leading order homogeneous elliptic equation on each coarse element. For a coarse rectangular element K, the basis functions ϕ_i, $i = 1, 2, 3, 4$, are computed via solution of:

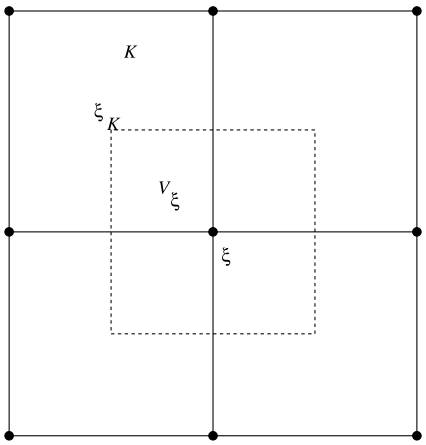

Fig. 1. Schematic of nodal points and grid.

$$\begin{aligned} \nabla \cdot (\mathbf{k} \cdot \nabla \phi_i) &= 0 \quad \text{in } K \\ \phi_i &= g_i \quad \text{on } \partial K, \end{aligned} \tag{2.6}$$

for prescribed boundary function g_i. Eq. (2.6) must be solved four times for the determination of the four ϕ_i. The basis function associated with the vertex $\mathbf{x}_i$ is constructed from the union of the basis functions that share this $\mathbf{x}_i$ and are zero elsewhere. Note that ϕ_i must satisfy $\phi_i(\mathbf{x}_j) = \delta_{ij}$.

Hou and Wu [20] showed that the accuracy of the resulting coarse model is impacted by the treatment of boundary effects in (2.6). Enhanced accuracy can be achieved by solving local one-dimensional problems [22] for the determination of g_i or, as is considered here, by solving (2.6) in a domain that includes more than just the fine scale cells corresponding to the coarse block K (this approach is referred to as oversampling). The specific boundary conditions that are used in this paper for the determination of the basis functions will be discussed in detail below. A vertex-centered finite volume procedure is used to solve (2.6).

As discussed in [17], once the basis functions are constructed we determine $p^h \in V^h$, where V^h is the space of the approximate pressure solution, with $p^h = \sum_{\mathbf{x}_j \in Z_h^0} p_j \phi_j$, by enforcing

$$\int_{\partial V_{\boldsymbol{\xi}}} (\lambda(S)\mathbf{k} \cdot \nabla p^h) \cdot \mathbf{n} \, \mathrm{d}l = \int_{V_{\boldsymbol{\xi}}} q \, \mathrm{d}\mathbf{x}, \tag{2.7}$$

for every control volume $V_{\boldsymbol{\xi}} \subset \Omega$. Here $\mathbf{n}$ defines the normal vector on the boundary of the control volume $\partial V_{\boldsymbol{\xi}}$ and S is the fine scale saturation. Note that the integral in (2.7) is performed over a coarse cell in the dual grid ($V_{\boldsymbol{\xi}}$) and the finite element test function is unity. For this reason, the technique is referred to as a finite volume element method. In this way the method differs from multiscale finite element procedures (e.g., [20]).

3. Flow based oversampling for multiscale finite element methods

First, we describe the oversampling technique. The procedure is as follows. Denote a target coarse block by K (we assume rectangular partition in 2D, for simplicity) and an extended coarse region by K' (see Fig. 2). For K' with vertices $\mathbf{y}_i$ ($i = 1, 2, 3, 4$), we denote by $\psi_i(\mathbf{x})$ a nodal basis on K', such that $\psi_i(\mathbf{y}_j) = \delta_{ij}$. These nodal basis functions ψ_i ($i = 1, 2, 3, 4$) are constructed by solving (2.6) in the region K' (see Fig. 2) with *linear boundary conditions*. Once the auxiliary functions ψ_i (also called oversampling functions) are constructed, we compute the basis functions ϕ_i as a linear combination of ψ_i (as is done in oversampling for MsFEM [20]) as follows:

$$\phi_i(\mathbf{x}) = \sum_{j=1}^{4} c_{ij} \psi_j(\mathbf{x}), \tag{3.1}$$

where $\mathbf{x}_j$ are the nodes of the target coarse block K and c_{ij} are coefficients determined by imposing $\phi_i(\mathbf{x}_j) = \delta_{ij}$. By this construction, the resulting multiscale basis functions

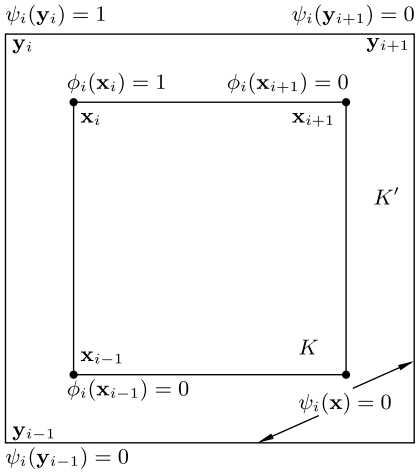

Fig. 2. Schematic description of coarse block and extended coarse block regions.

are nonconforming. Using these basis functions, the global problem is solved using (2.7). We emphasize that this method is not limited to rectangular global domain. In the case of non-rectangular domains, one can still use global auxiliary solutions with some generic boundary conditions. It is required that these auxiliary fields are linearly independent, so that one can construct linearly independent multiscale basis functions ϕ_i.

In our simulations, we are interested in taking the oversampled domain to be the entire region, i.e., $K' = \Omega$. This is in particular used for porous media without scale separation and strong non-local effects such as those considered in this paper. By taking the oversampling region to be the entire domain, one avoids typical resonance errors in numerical homogenization (see e.g., [20,18]). Associated with this is the global solutions corresponding to single-phase flow problems which are computed once. We refer to the *standard oversampling* technique when generic oversampling functions are used (as described above) for constructing multiscale basis functions.

In this work, we propose the use of flow based oversampling auxiliary functions for the construction of basis functions. This method differs from the standard oversampling method. In the flow based oversampling method, we replace some of the standard oversampling auxiliary functions (solutions of single-phase flow equations) by the ones obtained from solving the single-phase flow problem with the actual boundary conditions of two-phase flow. More precisely, if two-phase flow equation is solved subject to some boundary conditions, then we replace some of the generic oversampling auxiliary functions, ψ_j in (3.1), with oversampling functions with the boundary conditions as those in two-phase flow. Note that the standard oversampling assumes that the oversampling functions have linear boundary conditions. In applications, the boundary conditions are often non-smooth and can have an impact on the flow solutions. For this purpose, one needs to take into account non-smooth effects via auxiliary oversampling functions. Typical situations occur, for example, when the flow is corner-to-corner (see next section for details). In this case, the boundary conditions are no longer smooth and one of the oversampling functions is taken to be the solution of corner-to-corner flow.

We would like to remark that the computational time required for the standard oversampling and the flow based oversampling is similar. Indeed, in the flow based oversampling approach, some of the standard oversampling auxiliary functions are replaced by flow based single-phase flow solutions. The latter does not affect the computational time unless we need to incorporate many flow boundary conditions into the multiscale basis functions. However, the computational time required for flow based approaches is, generally, larger than that for local multiscale methods. Since in local approaches one still needs to solve the local problems over each coarse grid block, the total computational time can be similar to solving the global problems. This is, in particular, holds if the oversampling regions are larger than the target coarse grid blocks. We would like to stress again that the global solutions are computed offline for the calculation of multiscale basis functions. Note one can incorporate multiple global information in the flow based oversampling approach which is not the case in multiscale finite element method using limited global information introduced in [17,15].

3.1. Analysis

In this section, we show that the use of actual flow boundary conditions in oversampling methods is important. Consider the flow equations for two-phase flow in the form

$$-\nabla\cdot(\lambda(S)\mathbf{k}\cdot\nabla p) = 0,\ p|_{\Gamma_1} = g_{\mathrm{D}},\quad \frac{\partial p}{\partial n}|_{\Gamma_2} = g_{\mathrm{N}}; \tag{3.2}$$

where g_{D} and g_{N} may be discontinuous along the boundaries Γ_1, Γ_2. Let Q be the solution for the single phase flow equation,

$$-\nabla\cdot(\mathbf{k}\cdot\nabla Q) = 0,\qquad Q|_{\Gamma_1} = g_{\mathrm{D}},\ \frac{\partial Q}{\partial n}|_{\Gamma_2} = g_{\mathrm{N}}. \tag{3.3}$$

By using Eqs. (3.2) and (2.3) (with $h_{\mathrm{w}} = 0$), we can derive the equation for p:

$$\begin{aligned}-\nabla\cdot(\mathbf{k}\cdot\nabla p) &= -\frac{1}{\lambda(S)}\nabla\cdot(\lambda(S)\mathbf{k}\cdot\nabla p) - \frac{1}{\lambda(S)^2}\\ &\quad\times(\lambda(S)\mathbf{k}\cdot\nabla p)\cdot\lambda'(S)\nabla(S)\\ &= -\frac{\lambda'(S)}{\lambda(S)^2}\mathbf{v}\cdot\nabla(S) = \frac{1}{f'(S)}\left(\frac{1}{\lambda(S)}\right)_t\end{aligned} \tag{3.4}$$

with $p|_{\Gamma_1} = g$, $\frac{\partial p}{\partial n}|_{\Gamma_2} = g_{\mathrm{N}}$. Now let $w = p - Q$, and by subtracting Eqs. (3.2) and (3.4) we get

$$-\nabla\cdot(\mathbf{k}\cdot\nabla w) = \frac{1}{f'(S)}\left(\frac{1}{\lambda(S)}\right)_t,\qquad w|_{\Gamma_1} = 0,\quad \frac{\partial w}{\partial n}|_{\Gamma_2} = 0. \tag{3.5}$$

This shows the difference between p and Q satisfies the elliptic equation with nonzero source and homogeneous boundary condition. Therefore, if $\frac{1}{f'(S)}\left(\frac{1}{\lambda(S)}\right)_t$ has certain regularity, w can be approximated by generic solutions very well. Thus, $p = Q + w$, where w is a smooth function of two linearly independent solutions of single-phase flow equation as it was shown in [25]. This result further justifies the use of Q, the solution of single-phase flow with actual flow boundary conditions.

4. Numerical results

In this section, we present representative simulation results with quadratic relative permeabilities, $k_{\mathrm{rw}}(S) = S^2$ and $k_{\mathrm{ro}}(S) = (1-S)^2$. In all cases the system uses permeability fields from one of the layers in the benchmark test, the SPE comparative project [12] (upper Ness layers). These permeability fields are highly heterogeneous, channelized, and difficult to upscale. Fig. 3 depicts the log-permeability for one of the layers.

We employ the flow based multiscale finite volume element method for solving the pressure Eq. (2.2). The basis functions are constructed once and used throughout the simulations without updating them. The saturation Eq. (2.3) is solved on the fine grid using upwind finite volume method with flux limiter. For this purpose, the fine-scale velocity field is reconstructed from the multiscale basis functions representation of the pressure and via Darcy's Law.

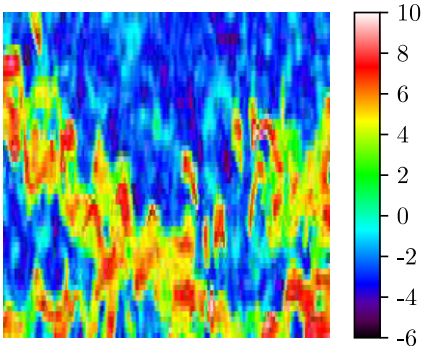

Fig. 3. Log-permeability for one of the layers of upper Ness.

Simulation results are presented for the saturation fields as well as total flow rate and the oil cut as a function of pore volume injected (PVI). The oil cut is also referred to as the fractional flow of oil. The oil cut (or fractional flow) is defined as the fraction of oil in the produced fluid and is given by q_{o}/q_t, where $q_t = q_{\mathrm{o}} + q_{\mathrm{w}}$, with q_{o} and q_{w} being the flow rates of oil and water at the production edge of the model. In particular, $q_{\mathrm{w}} = \int_{\partial\Omega^{\mathrm{out}}} f(S)\mathbf{v}\cdot\mathbf{n}\,\mathrm{d}\omega$, $q_t = \int_{\partial\Omega^{\mathrm{out}}} \mathbf{v}\cdot\mathbf{n}\,\mathrm{d}\omega$, and $q_{\mathrm{o}} = q_t - q_{\mathrm{w}}$, where $\partial\Omega^{\mathrm{out}}$ is the outer flow boundary. We use the notation Q for total flow q_t and F for fractional flow q_{o}/q_t in numerical results. Pore volume injected, defined as $\mathrm{PVI} = \frac{1}{V_{\mathrm{p}}}\int_0^t q_t(\tau)\,\mathrm{d}\tau$, with V_{p} being the total pore volume of the system, provides the dimensionless time for the displacement. When using multiscale finite volume element methods for two-phase flow, one can update the basis functions near the sharp fronts. Indeed, sharp fronts modify the local heterogeneities and this can be taken into account by resolving the local Eq. (2.6), for basis functions. If the saturation is smooth in the coarse block, it can be approximated by its average in (2.6), and consequently, the basis functions are not needed to be updated. It can be shown that this approximation yields first-order errors (in terms of coarse mesh size). In our simulations, we have found only slight improvement when the basis functions are updated, thus the numerical results for the MsFVEM presented in this paper do not include the basis functions update near the sharp fronts.

In all numerical examples, the fine-scale field is 220×60, while the coarse-scale field is 22×6. We have observed similar results for other coarse grids. The boundary condition is imposed by specifying $p = 1$, $S = 1$ along

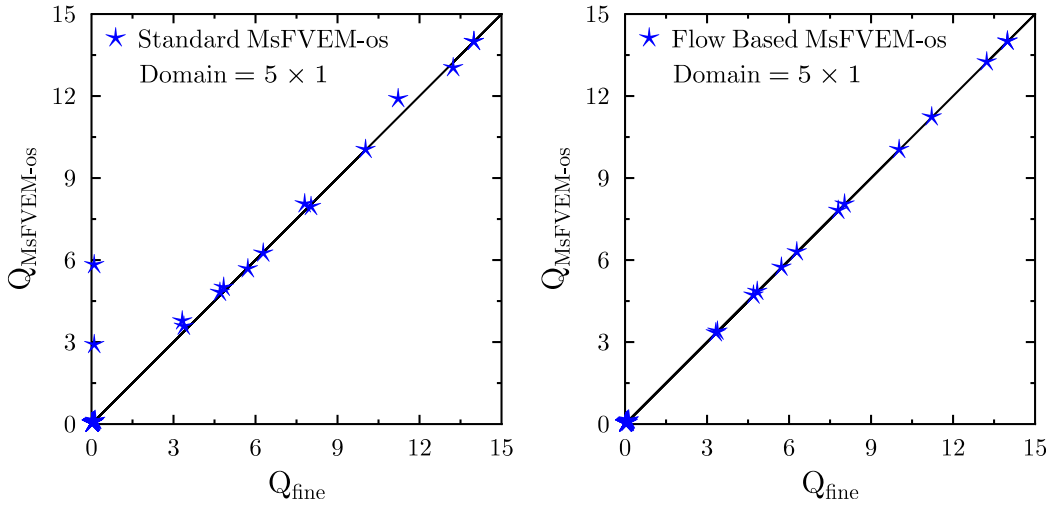

Fig. 4. Total single-phase flow rate for 50 layers of SPE 10 using the standard oversampling (left) and the flow based oversampling (right). Domain size is 5×1.

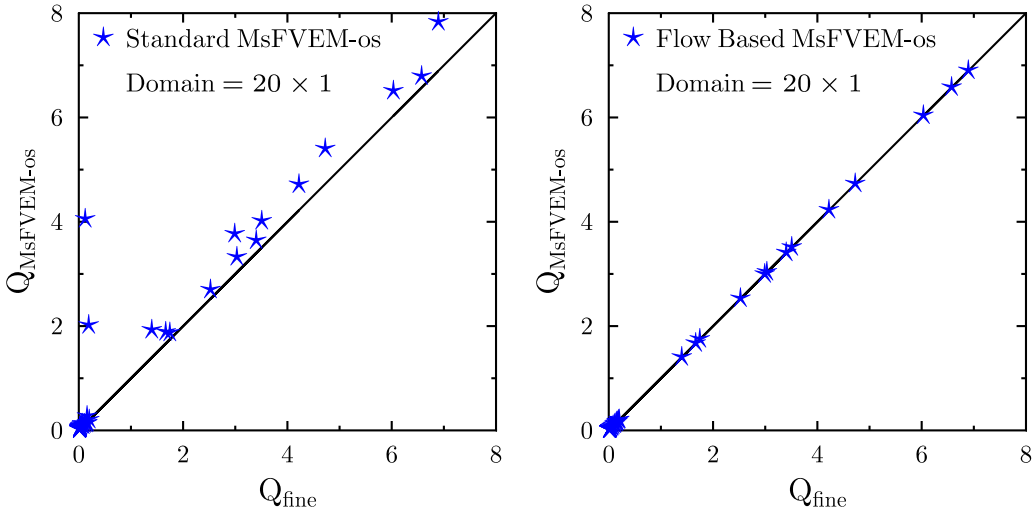

Fig. 5. Total single-phase flow rate for 50 layers of SPE 10 using the standard oversampling (left) and the flow based oversampling (right). Domain size is 20×1.

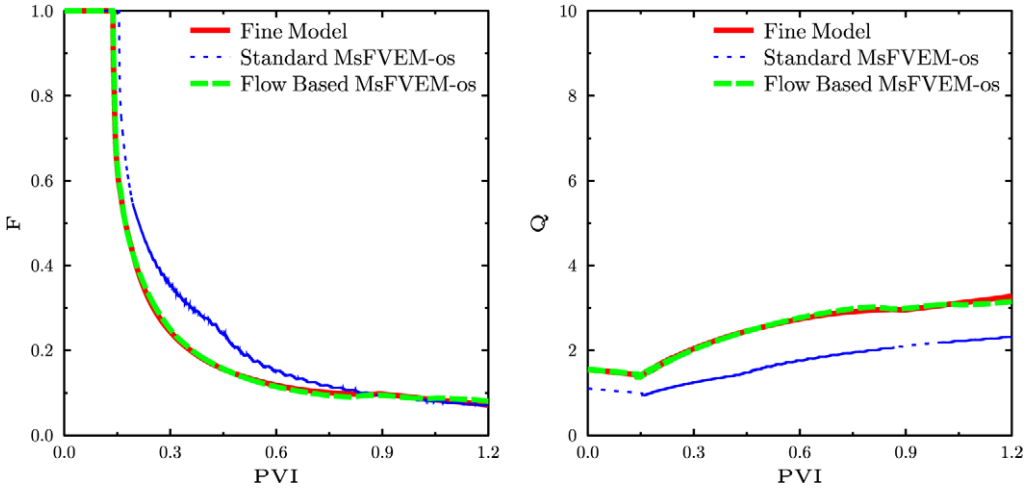

Fig. 6. Fractional flow (left figure) and total production (right figure) comparison for the standard oversampling and the flow based oversampling techniques. The viscosity ratio is $\mu_o/\mu_w = 5$.

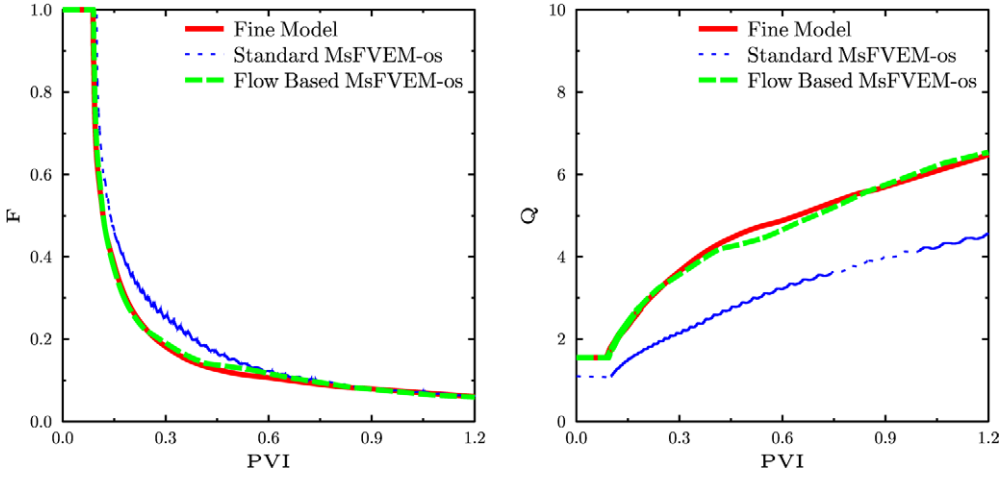

Fig. 7. Fractional flow (left figure) and total production (right figure) comparison for the standard oversampling and the flow based oversampling techniques. The viscosity ratio is $\mu_o/\mu_w = 15$.

the $x = 0$ edge for $0 \leqslant z \leqslant 0.1$ and $p = 0$ along the $x = L$ edge for $0.9 \leqslant z \leqslant 1$. On the rest of the boundaries, we assume no flow boundary condition. Here, L is the horizontal size of the global rectangular domain. We note that these boundary conditions are different from those used in constructing generic oversampling functions.

In our first numerical results, we compare the total flow rate Q for single-phase flow using the standard oversampling and the flow based oversampling methods. The global domain sizes are 5×1 (Fig. 4) and 20×1 (Fig. 5), i.e., $L = 5$ and $L = 20$, respectively. In both cases, we observe that the flow based oversampling gives nearly exact results, while standard oversampling methods are not as accurate. The accuracy of standard oversampling methods deteriorates as the anisotropy ratio increases.

Next, we present numerical results for dynamic quantities, such as fractional flow, total flow rate and saturation maps for two-phase flow and transport. In Figs. 6 and 7, we present the fractional flow ($F = q_o/q_t$, left figure) and the total flow ($Q = q_t$, right figure) for two viscosity ratio cases, $\mu_o/\mu_w = 5$ and $\mu_o/\mu_w = 15$. The solid line designates the fine-scale reference solution, while dotted line designates the standard oversampling method where generic global single-phase flow solutions are used, and dashed line designates the flow-based oversampling method. We observe from these figures that the flow based oversampling method is more accurate. This is more evident from the total flow plot. Next, we compare the saturation fields at different time instances. In Fig. 8, the saturation fields at the time instances, PVI $= 0.1, \ldots, 0.9$, are depicted. One

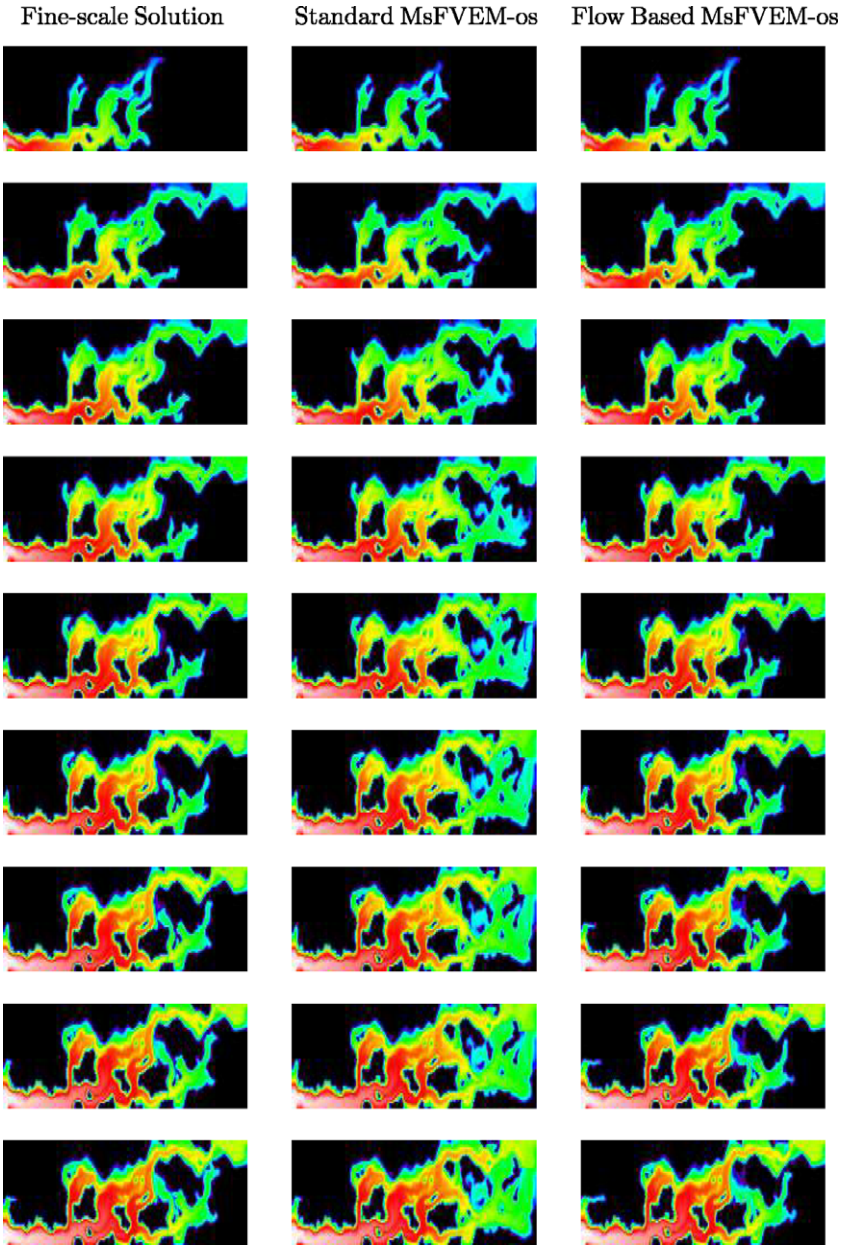

Fig. 8. Saturation maps at PVI=0.1–0.9 for fine-scale solution (left figure), standard MsFVEM-os (middle figure), and flow-based MsFVEM-os (right figure). Corner-to-corner boundary condition is used. Layer 61.

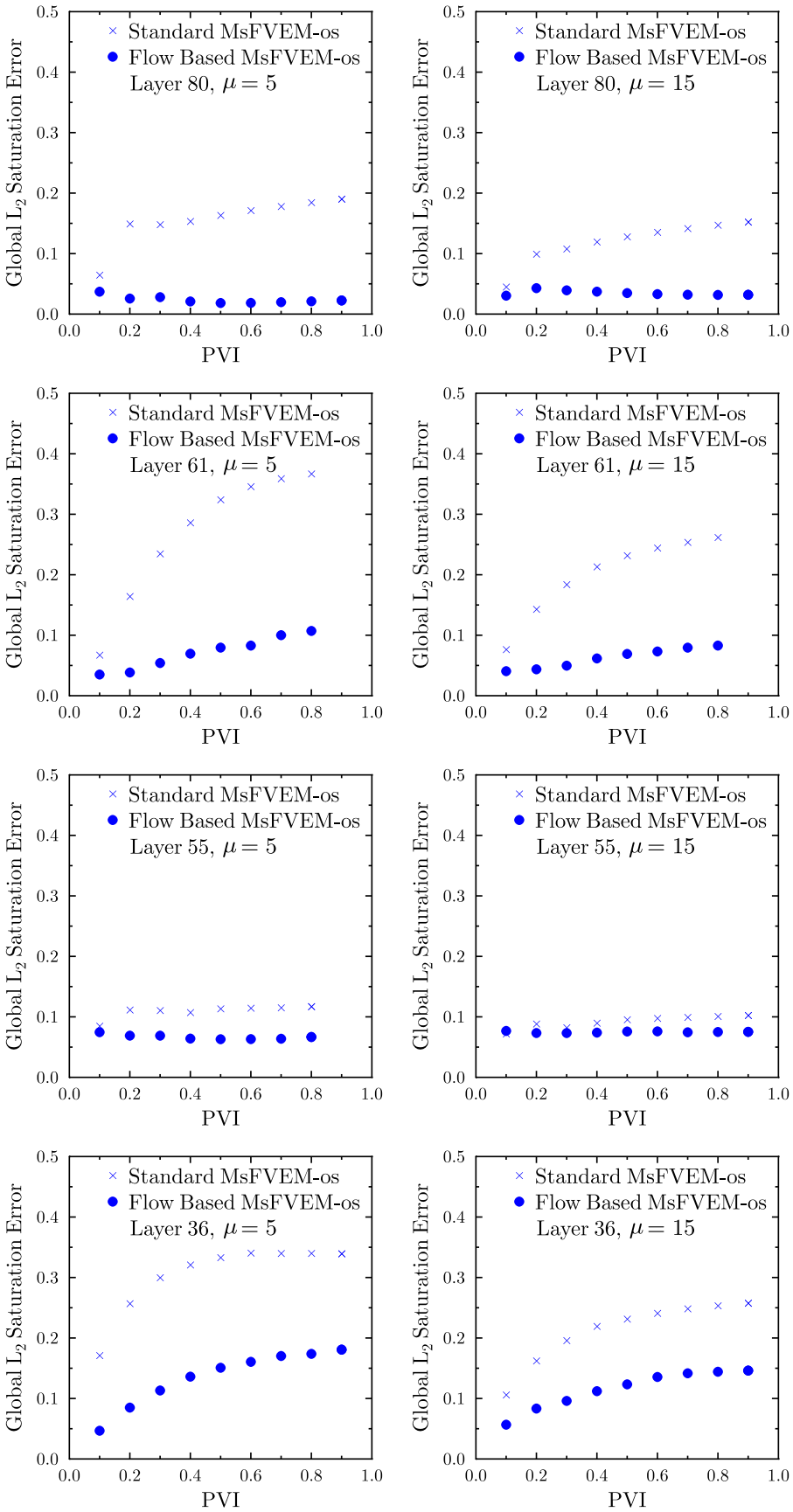

Fig. 9. L_2 saturation errors at different PVIs.

can observe that the saturation fields obtained from the standard oversampling method are not very accurate. This is more evident in the regions close to upper right corner.

To compare the saturation maps at different time instances quantitatively, we plot L_2 errors of the saturations fields in Fig. 9. In particular, we present these plots for four different layers of SPE 10 with two different viscosity ratios $\mu_0/\mu_w = 5$ (left figures) and $\mu_o/\mu_w = 15$ (right figures). The saturation errors are computed at $PVI = 0.1, 0.2, \ldots, 0.9$. We observe that the errors in saturation fields for the flow based oversampling techniques are smaller compared to the standard oversampling method in all cases. In most cases, the error is smaller by several factors. We note again that the cost of these computations are the same and involve computing four auxiliary oversampling functions. We have also tried numerical results with different boundary conditions where Dirichlet boundary conditions are imposed over two coarse grid blocks at $x = 0$ and $x = L$. In these cases, we have observed consistent improvement when the flow based oversampling method is used.

In the paper, we discussed the cases with singular type boundary conditions and assumed no source terms. The source terms representing well information are common in applications. One can consider singular source terms (such as Dirac δ functions) within the proposed framework. In this case, the flow based auxiliary functions will the global solutions containing the singular sources. We will present these results elsewhere.

5. Concluding remarks

In this paper, we study oversampling techniques for multiscale simulation of two-phase immiscible flow in heterogeneous porous media with strong non-local effects. We propose the flow based oversampling technique where the actual two-phase flow boundary conditions are used in constructing the oversampling functions. In our numerical simulations, the oversampling region is taken to be the entire domain due to strong non-local effects. We compare the proposed approach to standard oversampling technique which uses generic global boundary conditions that do not reflect the actual flow boundary conditions. The flow based oversampling approach replaces some of the global oversampling basis functions with the solutions of single-phase flow equation with actual two-phase flow boundary conditions. Our numerical results show that the second approach is several times more accurate in almost all the cases considered in the paper. We provide partial theoretical explanation for these numerical observations.

Acknowledgements

The authors gratefully acknowledge financial support from US DOE under Grant DE-FG02-06ER25727. We are grateful to reviewers whose comments greatly improved the paper.

References

[1] Aarnes J. On the use of a mixed multiscale finite element method for greater flexibility and increased speed or improved accuracy in reservoir simulation. SIAM MMS 2004;2:421–39.
[2] Aarnes J, Kippe V, Lie K-A. Mixed multiscale finite elements and streamline methods for reservoir simulation of large geomodels. Adv Water Resour 2005;28(3):257–71.
[3] Arbogast T. Implementation of a locally conservative numerical subgrid upscaling scheme for two-phase Darcy flow. Comput Geosci 2002;6:453–81. Locally conservative numerical methods for flow in porous media.
[4] Arbogast T, Pencheva G, Wheeler MF, Yotov I. A multiscale mortar mixed finite element method. SIAM J. Multiscale Model Simul. 2007;6(1):319–46.
[5] Babuška I, Caloz G, Osborn E. Special finite element methods for a class of second order elliptic problems with rough coefficients. SIAM J Numer Anal 1994;31:945–81.
[6] Babuška I, Osborn E. Generalized finite element methods: their performance and their relation to mixed methods. SIAM J Numer Anal 1983;20:510–36.
[7] Barker JW, Thibeau S. A critical review of the use of pseudo-relative permeabilities for upscaling. SPE Res Eng 1997;12: 138–43.
[8] Chen Y, Durlofsky LJ. Adaptive coupled local-global upscaling for general flow scenarios in heterogeneous formations. Transport Porous Med 2006;62:157–85.
[9] Chen Y, Durlofsky LJ, Gerritsen M, Wen XH. A coupled local-global upscaling approach for simulating flow in highly heterogeneous formations. Adv Water Resour 2003;26:1041–60.
[10] Chen Z, Hou TY. A mixed multiscale finite element method for elliptic problems with oscillating coefficients. Math Comp 2002;72: 541–76. Electronic.
[11] Christie M. Upscaling for reservoir simulation. J Pet Tech 1996:1004–10.
[12] Christie M, Blunt M. Tenth spe comparative solution project: a comparison of upscaling techniques. SPE Reser Eval Eng 2001;4:308–17.
[13] Durlofsky LJ. Numerical calculation of equivalent grid block permeability tensors for heterogeneous porous media. Water Resour Res 1991;27:699–708.
[14] Durlofsky LJ. Coarse scale models of two phase flow in heterogeneous reservoirs: volume averaged equations and their relationship to the existing upscaling techniques. Comput Geosci 1998;2: 73–92.
[15] Durlofsky LJ, Efendiev Y, Ginting V. An adaptive local-global multiscale finite volume element method for two-phase flow simulations. Advances in Water Resources. 2007;30:576–88.
[16] E W, Engquist B. The heterogeneous multi-scale methods. Comm Math Sci 2003;1(1):87–133.
[17] Efendiev Y, Ginting V, Hou T, Ewing R. Accurate multiscale finite element methods for two-phase flow simulations. J Comput Phys 2006;220:155–74.
[18] Efendiev Y, Hou T, Wu XH. Convergence of a nonconforming multiscale finite element method. SIAM J Numer Anal 2000;37: 888–910.
[19] Gerritsen M, Durlofsky L. Modeling of fluid flow in oil reservoirs. Ann Rev Fluid Mech 2005;37:211–38.
[20] Hou T, Wu XH. A multiscale finite element method for elliptic problems in composite materials and porous media. J Comput Phys 1997;134:169–89.
[21] Hughes T, Feijoo G, Mazzei L, Quincy J. The variational multiscale method – a paradigm for computational mechanics. Comput Meth Appl Mech Engrg 1998;166:3–24.
[22] Jenny P, Lee SH, Tchelepi H. Multi-scale finite volume method for elliptic problems in subsurface flow simulation. J Comput Phys 2003;187:47–67.
[23] Jenny P, Lee SH, Tchelepi H. Adaptive multi-scale finite volume method for multi-phase flow and transport in porous media. Multiscale Model Simul 2005;3:30–64.

[24] Matache A-M, Schwab C. Homogenization via p-FEM for problems with microstructure. In: Proceedings of the fourth international conference on spectral and high order methods (ICOSAHOM 1998), vol. 33. Herzliya; 2000. p. 43–59.
[25] Owhadi H, Zhang L. Metric based up-scaling. Comm Pure Appl Math 2006;60:675–723.
[26] Renard P, de Marsily G. Calculating effective permeability: a review. Adv Water Resour 1997;20:253–78.
[27] Sangalli G. Capturing small scales in elliptic problems using a residual-free bubbles finite element method. Multiscale Model Simul 2003;1:485–503. Electronic.
[28] Wen XH, Gomez-Hernandez JJ. Upscaling hydraulic conductivities in heterogeneous media: an overview. J Hydrol 1996;183: ix–xxxii.